

## Supercurrents through superconducting-normal-superconducting proximity layers.

### I. Analytic solution\*

H. J. Fink

Department of Electrical Engineering, University of California, Davis, California 95616

(Received 5 April 1976)

A general equation is derived for the maximum lossless current density which can be sustained through a thick normal layer which is part of a superconducting-normal-superconducting (SNS) sandwich. This result is adapted to nonuniform current densities and compared with experiments on Pb-Cu-Pb by Clarke. Agreement is obtained when the ratio of the pair potentials at the  $SN$  boundaries is made a constant, independent of temperature and thickness of the Cu layer. The pair potential in Cu is interpreted as an effective one which is induced in Cu by the proximity effect due to Pb. The superconducting phase difference is calculated across the  $N$  metal as a function of current for various thicknesses of the  $N$  layer. It reduces to the Josephson dc current relation when the  $N$  metal becomes thick in relation to the coherence length in the  $N$  region. We find that the value of the pair potential in the center of the  $N$  metal is current dependent and finite (not zero) for all current densities including the critical.

#### I. INTRODUCTION

It is known from experiments<sup>1-4</sup> that a triple layer consisting of superconductor-normal-metal-superconductor (SNS) can support a lossless dc supercurrent flowing perpendicular to the  $SN$  boundaries through the normal metal even when the normal metal is as thick as  $1 \mu\text{m}$ . The dc supercurrent density  $J_s$  has a maximum value  $J_c$ . Clarke<sup>2</sup> has shown experimentally that  $J_c = f(T)e^{-2d_n/k_n}$ , where  $f(T)$  is some function of temperature  $T$ ,  $d_n$  is the half-thickness of the  $N$  region, and  $k_n^{-1}$  is a decay length characteristic of the electronic properties of the  $N$  metal. These experiments<sup>2</sup> were performed at temperatures between the transition temperature  $T_c$  and less than  $0.2T_c$  with a clean  $S$  metal [mean free path  $l_s \gg \xi_s(T)$ , the coherence length of the  $S$  metal] and a dirty  $N$  metal ( $l_n \ll k_n^{-1}$ ) when  $2d_n k_n > 1$ . Bondarenko *et al.*<sup>3</sup> reach similar conclusions for a clean  $N$  metal.

From these experiments one may conclude that the  $N$  metal acquires superconducting properties when in contact with the  $S$  regions due to the proximity effect, since otherwise it is difficult to imagine that a supercurrent (phase current) may pass through the  $N$  metal without a dc potential difference across it. This implies that the electrochemical potential of the superconducting pairs  $\mu_p$  is constant and continuous throughout the SNS specimen parallel to the transport current across the SNS triple layer.

De Gennes<sup>5</sup> attacked the SNS problem from the theoretical point of view for both the  $S$  and  $N$  regions dirty and obtained the exponential thickness dependence of  $J_c$  and  $J_c \propto (T - T_c)^2$  for  $T$  close to  $T_c$ . However, as pointed out by Yamafuji *et al.*,<sup>6</sup> the boundary conditions at the  $SN$  interfaces as used by de Gennes lead to a discontinuous phase

current across the boundaries. In the very weak coupling limit de Gennes obtains<sup>5</sup> the Josephson<sup>7</sup> dc current-phase relation.

Jacobson<sup>8</sup> derived the Josephson dc relation<sup>7</sup> for a very thin oxide barrier using the Ginzburg-Landau<sup>9</sup> (GL) equations in the  $S$  regions and a quasitype Schrödinger-GL equation in the insulator in terms of barrier height and width. In his approach, the oxide behaves like a weak superconductor.

Microscopic calculations for SNS triple layers when the  $S$  and  $N$  regions are pure ( $l_s \rightarrow \infty$ ;  $l_n \rightarrow \infty$ ) were performed by Kulik<sup>10</sup> and revised by Ishii<sup>11</sup> for  $T = 0^\circ\text{K}$ . Ishii<sup>11</sup> found that the supercurrent density  $J_s$  is a linear function of the phase for phase differences between  $0$  and  $\pi$  and that  $J_c \propto d_n^{-1}$  for  $2d_n \gg \xi_0$  ( $\xi_0$  is that of the  $S$  region). Bardeen and Johnson<sup>12</sup> extended Ishii's calculations to temperatures above absolute zero by employing Galilean invariance to the quasiparticle spectrum in the  $N$  metal. References 10-12 assume that the effective electron masses and Fermi velocities are the same in the  $S$  and  $N$  regions and that the pair potential vanishes in the  $N$  region. This has the effect that in the final equations the contributions arising from the  $S$  and  $N$  regions separately are not readily distinguishable. Bardeen and Johnson<sup>12</sup> find that at absolute zero  $J_s$  changes linearly for phase differences  $\phi$  between zero and  $\pi$ . When the spacing between the bound quasiparticle states in the  $N$  metal and  $kT$  become comparable, they find<sup>12</sup> that  $J_s \propto \sin\phi$ . They also find that at  $\phi = \frac{1}{2}\pi$ , the value of  $J_s = a(d^*)^{-1}e^{2\alpha^*T}$ , where  $a$  and  $c$  are temperature-independent constants and  $2d^* = 2d_n + \pi\xi_0$ .

Baratoff *et al.*<sup>13,14</sup> and Yamafuji *et al.*<sup>6</sup> applied the GL theory<sup>9</sup> to weak links when the barrier is a superconductor in the superconducting state.

In Refs. 13 and 14 the amount of superconductivity in the barrier is weakened, for example, by having only a shorter mean free path in the barrier region as compared to the adjacent  $S$  regions, or by an actual physical constriction in the cross section. In Ref. 6, the values of  $T_c$  and  $H_c$ , the transition temperature and the thermodynamic critical field, are chosen to be smaller in the  $N$  region than in the outside  $S$  regions.

It is the purpose of this work to investigate in detail tunneling of superconducting pairs through a thick normal layer whose bulk transition temperature is very near absolute zero and to calculate the critical current density  $J_c(T)$ . We make no restrictions on the  $S$  and  $N$  regions as to clean or dirty limits. We assume that the SNS specimen is symmetric (both  $S$  regions are the same), that the thickness  $d_s \gg \xi_s$  in general and the thickness of the  $N$  region  $2d_n$  is arbitrary. Furthermore, the Fermi velocities  $v_{F_s}$  and  $v_{F_n}$ , the effective electron masses  $m_s$  and  $m_n$ , and mean free paths  $l_s$  and  $l_n$  are assumed to be distinctly different. It is assumed that the superconducting phase current density  $J_s$  is continuous at the  $SN$  boundaries and elsewhere and we express our final results in terms of one remaining, as yet unspecified, boundary condition. This boundary condition connects the tunneling properties of the superconducting pairs through the normal region to the proximity effect. By comparing the available experiments with the proposed calculations over a wide range of temperatures, we extract this boundary condition and its temperature dependence. An in-depth exact computer study for various material parameters and boundary conditions is planned as a future extension of this work.

## II. GINZBURG-LANDAU EQUATIONS IN THE $S$ AND $N$ REGIONS

Assuming that the complex order parameter  $\Psi$  can be written as

$$\Psi_s = F_s(\vec{r}) e^{i\phi_s(\vec{r})} = F_s(\vec{r}) \exp i \left( \chi_s + \frac{2e}{\hbar c} \int \vec{A} \cdot d\vec{r} \right), \quad (1)$$

where  $\phi_s$  and  $F_s$  are real, then the real part of the first GL equation is

$$\left[ 1 - \frac{F_s^2}{F_s^2(\infty)} + \xi_s^2 \nabla^2 - \left( \frac{m_s}{\hbar e} \right)^2 \xi_s^2 \frac{J_s^2}{F_s^4} \right] F_s = 0, \quad (2)$$

where  $\xi_s$  is the coherence length as defined in the *bulk* of the  $S$  metal. The supercurrent density  $J_s$  is

$$\vec{J}_s(\vec{r}) = \frac{e\hbar}{2m_s} \left[ \Psi_s^*(\vec{r}) \left( \frac{1}{i} \nabla - \frac{2e}{\hbar c} \vec{A}(\vec{r}) \right) \Psi_s(\vec{r}) + \text{c.c.} \right]. \quad (3)$$

It is proposed that the  $N$  region in a SNS sandwich can be treated like a superconductor at least as long as a lossless supercurrent flows through it. This assumption is supported by the experimental facts as discussed in the Introduction.<sup>1-4</sup> Such a SNS structure has a collective transition temperature  $T_c$ . It is suggested that when  $d_n \gg \xi_n$  the collective  $T_c$  is a meaningful quantity provided the measuring current density is smaller than a certain critical current density  $J_c$  and fluctuations are not sufficient to break the long-range coherence. The current density in the  $N$  region is by analogy with Eq. (3)

$$\vec{J}_n(\vec{r}) = \frac{e\hbar}{2m_n} \left[ \Psi_n^*(\vec{r}) \left( \frac{1}{i} \nabla - \frac{2e}{\hbar c} \vec{A}(\vec{r}) \right) \Psi_n(\vec{r}) + \text{c.c.} \right]. \quad (4)$$

Assuming that the  $x$  direction is parallel to the current flow and the superconductive phase current is continuous at the  $SN$  boundary which is located at  $x = x_1$  (see insert of Fig. 1), it follows from Eqs. (3) and (4) that

$$\frac{F_s}{m_s} \frac{dF_s}{dx} \Big|_{x_1} = \frac{F_n}{m_n} \frac{dF_n}{dx} \Big|_{x_1} \quad (5)$$

and

$$\frac{1}{m_s} F_s^2 \frac{d\chi_s}{dx} \Big|_{x_1} = \frac{1}{m_n} F_n^2 \frac{d\chi_n}{dx} \Big|_{x_1}, \quad (6)$$

where  $\chi_s$  is defined in Eq. (1) and  $\Psi_n$ ,  $F_n$ , and  $\chi_n$  are defined by an equivalent equation. In the  $N$

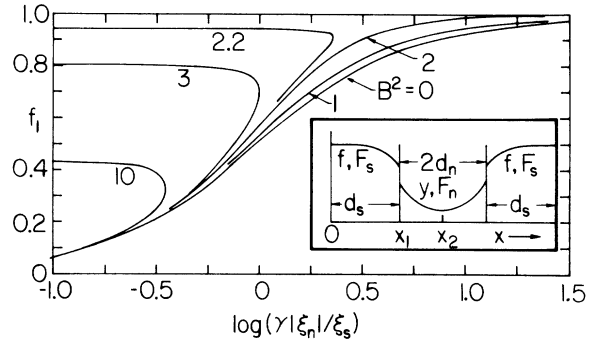


FIG. 1. Shown are solutions of Eq. (30) for constant values of  $b \equiv B^2$  [Eq. (12)].  $f_1$  is the normalized order parameter [Eq. (9)] at the  $SN$  boundary in the  $S$  metal located at  $x_1$  (see insert),  $\gamma$  is defined by Eq. (11) or (5a) and  $|\xi_n|/\xi_s = |\alpha|^{-1}$  by Eq. (14) and Eqs. (37), (41), or (44). When the temperature  $T \rightarrow T_c$ , the value of  $\log(\gamma |\xi_n|/\xi_s) \ll 0$  and when  $T \rightarrow T_{c_n}$  the  $\log(\gamma |\xi_n|/\xi_s) \gg 0$ .  $B = (|\Delta_{G_n}|/|\Delta_{G_s}|)_{x_1}$  is a measure of the match of the pair potentials at the  $SN$  interface. The base of the logarithm is 10.

region the equation equivalent in Eq. (2) may be written assuming  $J_n = J_s$ :

$$\left[1 - \frac{F_n^2}{F_n^2(\infty)} + \xi_n^2 \nabla^2 - \left(\frac{m_n}{\hbar e}\right)^2 \xi_n^2 \frac{J_s^2}{F_n^4}\right] F_n = 0. \quad (7)$$

Equation (7) shows the following: In the center of the  $N$  region, at  $x = x_2$ , one would expect that  $F_n^2/F_n^2(\infty)$  is very small compared to unity when the  $N$  region is thick, and by symmetry  $F_n^2(x)$  is a minimum there. Therefore,  $d^2F/dx^2$  must be larger than zero in the center of the  $N$  region at  $x = x_2$  (see insert of Fig. 1). When the transport current is zero, for example, one can readily see from Eq. (7) that  $\xi_n^2$  must be negative, or the *bulk* coherence length  $\xi_n$  must be imaginary. This is compatible with an  $N$  metal whose bulk transition temperature is very close to absolute zero. If one were to apply Eq. (7) to the  $N$  metal in bulk form above its transition temperature  $T_{cn}$ , isolated from the  $S$  regions, the only reasonable solution is  $F_n = 0$ . When the  $N$  metal is in contact with the  $S$  metal, however, superconductivity is induced in the  $N$  metal due to the proximity effect,  $F_n^2$  becomes larger than zero everywhere and its transition temperature becomes the collective  $T_c$  of the SNS sandwich. In effect,  $F_n^2$  is controlled by  $F_s^2$  through the boundary conditions at  $x_1$ . However,  $\xi_n$  remains that of the *bulk*, by definition, and is governed by  $T_{cn}$ .

Gor'kov<sup>15</sup> has related the complex order parameter  $\Psi_s$  to the pair potential  $\Delta_{Gs}$  by

$$\Psi_s \equiv \left[\frac{7}{8} \zeta(3) m_s \chi_{Gs}\right]^{1/2} (\Delta_{Gs} / \pi k T_c), \quad (8)$$

where  $n_s$  is the total electron density and  $\chi_{Gs}(T, l_s)$  is a function<sup>15</sup> of temperature and mean free path of the electrons. We postulate that a similar equation exists for  $\Psi_n$ . This postulate is not necessary in what follows below except that it is convenient for the interpretation of the boundary conditions at  $x_1$ .

We would like to point out, however, that  $\Delta_{Gn}$  is an effective pair potential<sup>16</sup> near the SN boundary, induced by the proximity effect, and not that of the  $N$  metal far away from the SN boundary (in the bulk). To understand this we suggest the following interpretation: Pairs diffuse or tunnel from the superconductor into the normal metal while normal-like electrons move in the opposite direction such that in the time average charge neutrality will be conserved. Since pairs cannot breakup instantaneously into single electrons in the  $N$  metal and single electrons cannot pair instantaneously in the  $S$  metal, the pairs will carry with them in the  $N$  metal the memory of the  $[N(0)V]_s$  interaction which will be retained for a certain time regardless of what the intrinsic bulk  $[N(0)V]_n$

interaction of the new host metal is, even when the latter is zero.  $N(0)$  is the local density of states per unit energy and per unit volume at the Fermi level and  $V$  is the effective BCS electron-phonon interaction constant. Thus, in the time average a reduced number of pairs will live in the  $N$  metal paired by the  $[N(0)V]_s$  interaction and the exact number density depends on the rate with which they are supplied to the  $N$  region by the  $S$  region and the rate with which they breakup, thus giving rise in the time average to an effective decay length  $|\xi_n|$  in the  $N$  region.

For the purpose of normalization of Eqs. (2), (5), and (7) we normalize the distance  $x$  by  $\xi_s$  in both the  $S$  and  $N$  regions and introduce the following definitions:

$$f \equiv F_s(x/\xi_s)/F_s(\infty), \quad (9)$$

$$y \equiv \left(\frac{n_s \chi_{Gs}}{n_n \chi_{Fn}}\right)^{1/2} \frac{F_n(x/\xi_s)}{F_s(\infty)} = \frac{|\Delta_{Gn}|}{|\Delta_{Gs}(\infty)|}, \quad (10)$$

$$\gamma \equiv (m_n/m_s)(F_s^2/F_n^2)|_{x_1}, \quad (11)$$

$$b \equiv B^2 \equiv (y^2/f^2)|_{x_1} = (|\Delta_{Gn}|^2/|\Delta_{Gs}|^2)|_{x_1}, \quad (12)$$

$$\gamma b \equiv \frac{m_s n_s \chi_{Gs}}{m_n n_n \chi_{Gn}} = \frac{dy^2/dx}{df^2/dx} \Big|_{x_1}, \quad (5a)$$

$$i \equiv \frac{m_s \xi_s}{\hbar |e| F_s^2(\infty)} J_s = \frac{4\pi}{c} \frac{\lambda_s}{\sqrt{2} H_c} J_s, \quad (13)$$

$$\alpha \equiv \xi_s^2/\xi_n^2, \quad (14)$$

$$I^2 \equiv -[(b\gamma)^2/\alpha]i^2, \quad (15)$$

$$z^2 \equiv -\alpha(x/\xi_s)^2. \quad (16)$$

For our problem the  $N$  metal is not superconducting in the bulk at temperatures which are of concern to us and, therefore,  $\alpha < 0$  since  $\xi_n^2 < 0$ . Hence  $I^2$  and  $z^2$  are positive. Equation (5a) corresponds to the boundary condition (5) and the definitions  $\gamma$  and  $b$  are the matching conditions for  $F$  and  $\Delta_G$  at  $x_1$ , the values of which are undetermined for the time being.

The one-dimensional, normalized equations corresponding to Eqs. (2) and (7) are

$$\frac{d^2 f}{dx^2} + \left(1 - f^2 - \frac{i^2}{f^4}\right) f = 0 \text{ for } S \text{ regions}, \quad (2a)$$

$$-\frac{d^2 y}{dz^2} + \left(1 - y^2 + \frac{I^2}{y^4}\right) y = 0 \text{ for } N \text{ region}. \quad (7a)$$

The SNS problem can be solved by solving Eqs. (2a) and (7a) with the boundary conditions (5a) and (12). The three parameters  $\alpha$ ,  $b$ , and  $\gamma b$  are governing the solutions of  $f$  and  $y$  for a fixed value of  $i$ .  $\alpha$  and  $\gamma b$  are temperature-dependent-materials parameters. The one-dimensional form of Eqs. (2a) and (7a) implicitly assumes that the current densities are uniform over the cross sec-

tions of the  $S$  and  $N$  regions. The negative sign in front of  $d^2y/dz^2$  guarantees that at  $x_2$  the function  $y$  has a minimum, and the positive sign in front of  $I^2$  is essential in obtaining a maximum lossless current for a given SNS structure as will become apparent below.

### III. SOLUTIONS OF EQS. (2a) AND (7a) FOR $N$ THICK

We shall solve first Eq. (7a) with the coordinates as shown in the insert of Fig. 1.  $y$  is symmetric with respect to  $x_2$ , the center of the  $N$  region, where  $y(x_2) \equiv y(z_2) \equiv y_2$ . The  $SN$  boundary is at  $y(x_1) \equiv y(z_1) \equiv y_1$ . When Eq. (7a) is integrated once with the boundary condition  $dy/dz = 0$  at  $z_2$ , the result is

$$\left(\frac{dy}{dz}\right)^2 = 2(y^2 - y_2^2) \left( y^2(2 - y_2^2 - y^2) + \frac{2I^2}{y_2^2} \right). \quad (17)$$

Introducing the new variable  $\psi_n^2 \equiv y^2 - y_2^2$  this becomes

$$\sqrt{2} \frac{d\psi_n}{dz} = [(\psi_n^2 + a_n^2)(b_n^2 - \psi_n^2)]^{1/2}, \quad (17a)$$

with

$$a_n^2 = -\left(1 - \frac{3}{2}y_2^2\right) + \left[\left(1 - \frac{1}{2}y_2^2\right)^2 + 2I^2/y_2^2\right]^{1/2}, \quad (18)$$

$$b_n^2 = +\left(1 - \frac{3}{2}y_2^2\right) + \left[\left(1 - \frac{1}{2}y_2^2\right)^2 + 2I^2/y_2^2\right]^{1/2}. \quad (19)$$

When Eq. (17a) is integrated<sup>17</sup> between the limits  $z$  and  $z_2$ , one obtains a solution which is a Jacobi elliptic function:

$$y^2 - y_2^2 = b_n^2 m_{1n} s^2(u | m_n), \quad (20)$$

where  $m_n$  is defined<sup>17</sup> as the *parameter* ( $0 \leq m_n \leq 1$ ) and  $m_{1n} = 1 - m_n$ .  $m_{1n}$  and  $u$  are defined by

$$m_{1n} = \frac{a_n^2}{a_n^2 + b_n^2} = \frac{1}{2} \left( 1 - \frac{1 - \frac{3}{2}y_2^2}{\left[\left(1 - \frac{1}{2}y_2^2\right)^2 + 2I^2/y_2^2\right]^{1/2}} \right), \quad (21)$$

$$u = \left[\frac{1}{2}|\alpha|(a_n^2 + b_n^2)\right]^{1/2}(x_2 - x). \quad (22)$$

Consider the case for which  $N$  is thick and the normalized critical current  $I_c \gg I \rightarrow 0$ . One would expect that  $1 \gg y_2 \neq 0$ , provided phase coherence exists within the  $N$  region. Then  $m_{1n} \simeq \frac{1}{2}y_2^2 \ll 1$ ,  $b_n^2 \rightarrow 2$ ,  $\frac{1}{2}(a_n^2 + b_n^2) \rightarrow 1$ . Furthermore, if we assume that a current  $I < I_c$  is flowing through the  $N$  region, one would expect that  $y_2(I=0) > y_2(I \neq 0) \neq 0$ . Since the  $m_{1n}$  value cannot change drastically for a fixed SNS structure with and without a current,  $m_{1n}$  will remain small compared to unity and the term  $I^2/y_2^2$  must be in general of the same order of magnitude or smaller than  $y_2^2$ . Hence  $y_2^2$  must be a function of  $I$ .

Neglecting terms of order  $y_2^4$  and smaller in Eq. (21) one obtains in the limit that  $N$  is thick:

$$I^2/y_2^2 = (2m_{1n} - y_2^2). \quad (21a)$$

One can see from Eq. (21a) that  $I^2$  reaches a maximum value  $I_c^2$  when  $y_{2c}^2 = m_{1n}$ . From this it follows that  $I_c = m_{1n}$ . As mentioned at the end of Sec. II, and as can be seen from Eq. (21a), a maximum value of  $I^2$  would not exist if one were to reverse the sign in front of  $I^2$  in Eq. (7a) and consequently also in Eq. (21a). Furthermore, in the thick limit,  $y_1^2 \gg y_2^2$  and  $u_1 = \sqrt{|\alpha|}d_n > 1$ . It then follows from Eq. (20), neglecting terms of order  $(m_{1n} \sinh 2u_1)^2$  and smaller, that  $(m_n - 1)$

$$y_1^2 = 2m_{1n} [\cosh^2 u_1 (1 - \frac{1}{4}m_{1n} \sinh 2u_1) - 1] \quad (20a)$$

or

$$I_c = m_{1n} \simeq 4e^{-2u_1} [1 - (1 - y_1^2)^{1/2}]. \quad (23)$$

As can be seen from Eq. (21a), the value of  $y_2$  depends sensitively on the current  $I$ , whereas  $y_1$  is essentially independent of  $I$  in the *thick* limit. Equation (23) is the critical current in terms of the thickness of the  $N$  layer and the value of the order parameter in the  $N$  region at the  $SN$  boundary.

We now proceed and solve Eq. (2a) for the order parameter  $f$  in the  $S$  region. When Eq. (2a) is integrated once one obtains with the boundary condition  $df/dx = 0$  at  $x = 0$  and the definition  $f(x=0) \equiv f_0$  (see insert of Fig. 1):

$$\left(\frac{df}{dx}\right)^2 = 2(f_0^2 - f^2) \left( f^2(2 - f_0^2 - f^2) - \frac{2I^2}{f_0^2} \right). \quad (24)$$

With  $\psi_s^2 \equiv f_0^2 - f^2$  Eq. (24) can be cast into the same form as Eq. (17a) which leads to a solution similar to Eq. (20):

$$f_0^2 - f^2 = b_s^2 m_{1s} s^2(u | m_s), \quad (25)$$

with

$$m_{1s} = 1 - m_s = a_s^2 / (a_s^2 + b_s^2), \quad (26)$$

$$u = \left[\frac{1}{2}(a_s^2 + b_s^2)\right]^{1/2} x, \quad (27)$$

$$a_s^2 = +\left(1 - \frac{3}{2}f_0^2\right) + \left[\left(1 - \frac{1}{2}f_0^2\right)^2 - 2I^2/f_0^2\right]^{1/2}, \quad (28)$$

$$b_s^2 = -\left(1 - \frac{3}{2}f_0^2\right) + \left[\left(1 - \frac{1}{2}f_0^2\right)^2 - 2I^2/f_0^2\right]^{1/2}. \quad (29)$$

When the  $S$  region is thick ( $d_s \gg 1$ ), the value of  $f_0^2$  will depend on the current density, hence on  $2d_n$ . When  $2d_n \rightarrow 0$  the value of  $f_0^2 \rightarrow \frac{2}{3}$  at  $J_c$ , and when  $\sqrt{|\alpha|}d_n \gg 1$ , the value  $f_0 \rightarrow 1$  for all super-current densities.

### IV. MATCHING OF BOUNDARY CONDITIONS AND CRITICAL CURRENT

If we assume that both  $S$  and  $N$  are thick, then the value of  $f_0 \rightarrow 1$  and  $y_2 \ll 1$ . Since for a thick  $N$  region the critical current (maximum lossless dc current) is very small and therefore cannot

have any effect upon the values of  $f$  and  $y$  at the  $NS$  boundaries, one may neglect the current terms in Eqs. (17) and (24) when applying these to the boundary condition (5a) at  $x_1$ . With the definition Eq. (12) one obtains an equation for  $f_1$  in terms of  $\alpha$ ,  $b$ , and  $\gamma$ . The solution is

$$f_1^2 = \frac{\gamma^2/|\alpha| + 1 \pm [(\gamma^2/|\alpha|)(2-b) + 1]^{1/2}}{\gamma^2/|\alpha| + b}. \quad (30)$$

A plot of  $f_1$  as a function of  $\gamma/\sqrt{|\alpha|} = \gamma|\xi_n|/\xi_s$  for constant  $b$  values is shown in Fig. 1.

The critical current density, Eq. (23), when cast into electrostatic units (esu) [ $\phi_0 = 2.068 \times 10^{-7}$ ], is

$$J_c = \frac{c\phi_0}{2\pi^2\lambda_s^2|\xi_n|} \frac{1}{\gamma b} [1 - (1 - bf_1^2)^{1/2}] e^{-2d_n/|\xi_n|}, \quad (31)$$

where  $f_1$  is given by Eq. (30),  $\gamma b$  by Eq. (5a), and  $b$  by Eq. (12).  $\gamma b$  and  $|\alpha|$  are temperature-dependent-material parameters. In one extreme limit when  $T \rightarrow T_c$ , the value of  $\xi_s \rightarrow \infty$  and therefore  $\log(\gamma|\xi_n|/\xi_s) \rightarrow -\infty$ . The other extreme is the limit  $T \rightarrow T_{cn}$ . Then  $|\xi_n| \rightarrow \infty$  and  $\log(\gamma|\xi_n|/\xi_s) \rightarrow +\infty$ . As can be seen from Fig. 1, this span of temperatures can be traversed only if  $B^2 = b < 2$ .

It also follows from Fig. 1 that  $f_1^2 \rightarrow 1$  for the low-temperature limit. In that limit  $J_c$  [Eq. (31)] would become imaginary unless  $b \leq 1$ . We therefore assume quite generally that  $b \leq 1$ . The meaning of the latter statement is that  $|\Delta_{cn}| \leq |\Delta_{cs}|$  at the  $NS$  boundary at  $x_1$ . This is very reasonable for temperatures for which the corresponding  $N$  metal in bulk form is in the normal state. In the limit that  $T \rightarrow T_c$  it follows from Eq. (30) that  $f_1 \rightarrow \gamma|\xi_n|/2\xi_s \ll 1$  and therefore, when  $f_1$  is substituted into Eq. (31) one finds  $J_c \propto (\Delta T)^2$ . In the other extreme when  $bf_1^2 \rightarrow 1$  the critical current density  $J_c \propto (\Delta T)$  as for an  $SIS$  ( $I$  is an insulator) Josephson junction.

If the value of  $b$  were known for given materials parameters,  $\gamma$  would also be known from Eq. (5a). Since  $|\alpha|$  is also known at a given temperature,  $f_1$  can be obtained from Eq. (30) or Fig. 1. This means that in an ideal situation,  $J_c$  is uniquely determined from Eq. (31) without any adjustable parameters. Unfortunately,  $b$  is not known with certainty. It is determined by the microscopic boundary conditions of the Gor'kov pair potential  $\Delta_c$  at  $x_1$ . Therefore  $J_c$ , when calculated from Eq. (31), depends on  $b$  for a given set of materials parameter. Hence, one should be able to determine the microscopic boundary conditions when comparing Eq. (31) with good experiments. In an ideal situation a good experiment constitutes an  $SNS$  specimen which has a small enough cross-sectional area such that the current density is

uniform. It also implies, even more importantly, that the evaporation of the  $S$  and  $N$  layers is clean enough that impurities at the  $SN$  interface, such as a thin oxide layer, will not change the microscopic boundary conditions sufficiently to influence the critical current density. Only in the latter instance can the microscopic boundary conditions be applied meaningfully to an experiment.

## V. CURRENT PHASE RELATION

The total phase difference of the superconducting phase across the  $SNS$  sandwich is

$$2 \int_{x=0}^{x_2} d\chi = -2 \int_{x=0}^{x_1} \frac{i}{f^2} dx - 2\gamma b \int_{x_1}^{x_2} \frac{i}{y^2} dx, \quad (32)$$

where the second term on the right-hand side is the total phase difference  $2(\chi_2 - \chi_1)$  across the  $N$  region (see insert of Fig. 1 for coordinates). In Eq. (32) the value of  $i$  is that of Eq. (13) and  $f$  and  $y$  are defined by Eqs. (9) and (10). The phase  $\chi$  is defined by Eq. (1) for the  $S$  regions, and by a similar equation for the  $N$  region.  $\gamma b$  is given by Eq. (5a). Equation (32) is the actual total phase difference  $\chi$  between two points and it should be noted that the definition of the phase difference in Refs. 8, 13, and 14 is not the same. There<sup>8,13,14</sup> the phase difference is defined as the phase difference between solutions for a constant supercurrent density  $J_s$  with and without the weak link ( $N$  region).

In this section we shall be concerned with the phase difference  $2(\chi_2 - \chi_1)$  across the  $N$  region only:

$$\chi_2 - \chi_1 = -\gamma b i \int_{x_1}^{x_2} \frac{dx}{y^2 + b_n^2 m_{1n} s d^2 [u(x)|m_n]}, \quad (33)$$

where  $y^2$  from Eq. (20) was substituted.

When one integrates<sup>18</sup> Eq. (33) one obtains

$$\chi_2 - \chi_1 = -\frac{\gamma b i}{n y_2^2 \left[ \frac{1}{2} |\alpha| (a_n^2 + b_n^2) \right]^{1/2}} \times \{ m_n u_1 + (n - m_n) \Pi [n; u_1 | m_n] \}, \quad (33a)$$

where  $a_n$ ,  $b_n$ , and  $m_n = 1 - m_{1n}$  are defined by Eqs. (18), (19), and (21),  $u_1 = d_n \left[ \frac{1}{2} |\alpha| (a_n^2 + b_n^2) \right]^{1/2}$  and  $n = m_n - b_n^2 m_{1n} / y_2^2$ .  $\Pi [n; u_1 | m_n]$  is an incomplete elliptic integral of the third kind. Equation (33a) is an *exact* solution of  $\chi_2 - \chi_1$  for arbitrary thicknesses  $2d_n$  of the  $N$  metal.

When the thickness of the  $N$  region is larger than  $\xi_n$ , then  $u_1 > 0.5$ ;  $m_n \rightarrow 1$ ;  $\frac{1}{2}(a_n^2 + b_n^2) \rightarrow 1$ ;  $b_n^2 \rightarrow 2$ ; and  $\Pi [n; u_1 | m_n \rightarrow 1]$  approaches the value given by Eq. (111.04), Ref. 18.

When Eq. (21a) is solved for  $y_2^2$  with  $m_{1n} = I_c$  one obtains

$$y_2^2 = I_c \{ 1 \pm [1 - (I/I_c)^2]^{1/2} \}. \quad (32b)$$

When the latter equation is substituted into Eq. (33a) with the above approximations for  $m_n - 1$ , one obtains for the phase difference across one-half the  $N$  region:

$$\chi_2 - \chi_1 = -\arctan \frac{(I/I_c) \tanh d_n \sqrt{|\alpha|}}{1 \pm [1 - (I/I_c)^2]^{1/2}}, \quad (33b)$$

where  $d_n \sqrt{|\alpha|}$  in conventional units is  $d_n / |\xi_n|$ . Figure 2 is a plot of Eq. (33b) for various thicknesses  $d_n \sqrt{|\alpha|}$ . When the  $N$  region is sufficiently thick  $\tanh d_n \sqrt{|\alpha|} \rightarrow 1$  and in this limit Eq. (33b) reduces to

$$I/I_c = -\sin[2(\chi_2 - \chi_1)]. \quad (33c)$$

This is the Josephson dc current relation<sup>7</sup> which is obtained in the very weak coupling limit.

In this limit the phase difference  $|2(\chi_2 - \chi_1)|$  across the  $N$  region approaches  $\frac{1}{2}\pi$  at the critical current, and it is smaller than  $\frac{1}{2}\pi$  at the critical current when the  $N$  region becomes thin and the phases between the superconducting regions couple more strongly (see Fig. 2). This conclusion does not take into account any phase differences in the  $S$  regions. For a fixed thickness of the  $N$  region there are two solutions for  $2(\chi_2 - \chi_1)$  for the same

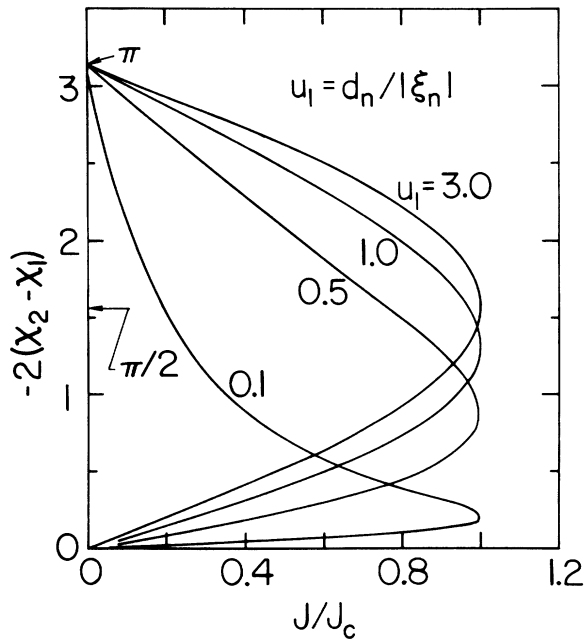


FIG. 2. Shown is the phase difference of the order parameter across the normal region as a function of supercurrent for various thicknesses of the  $N$  layer [Eq. (33b)].  $d_n$  is the half-thickness of the  $N$  region (see insert of Fig. 1). The curve for  $u_1 = 0.1$  lacks accuracy, since it is somewhat outside the range of our approximation. When  $d_n / |\xi_n| > 1.5$  the very weak coupling limit is reached which leads to the Josephson dc current relation [Eq. (33c)].

current. The *lower* branch in Fig. 2 is expected to be stable. Similarly,  $y_2^2$  has also two branches [Eq. (21b)]. The *upper* branch [positive sign in front of the square root of Eq. (21b)] is the stable branch for  $y_2^2$  and corresponds to the smaller phase differences in Fig. 2 for a given current density. Whatever the thickness of the  $N$  region may be, the values of  $|2(\chi_2 - \chi_1)|$  are always zero and  $\pi$  at  $I = 0$  and the corresponding  $y_2^2$  values are  $2I_c$  and zero. This means that when  $|2(\chi_2 - \chi_1)| = \pi$  the order parameter is zero in the center of the  $N$  region and it behaves similarly to that of an Abrikosov vortex when cut through its center. A phase difference of  $\pi$  is then sustained across the point where the order parameter is zero. However it should be realized that at the maximum current density the order parameter in the center of the  $N$  region *does not become zero*, but has a finite value  $y_2 = \sqrt{I_c}$  in normalized units [see Eq. (21b)]. Furthermore, the slopes of  $-2(\chi_2 - \chi_1)$  with respect to  $I/I_c$  for  $I \rightarrow 0$  are  $\tanh d_n \sqrt{|\alpha|}$  and  $-\coth d_n \sqrt{|\alpha|}$  at  $-2(\chi_2 - \chi_1) = 0$  and  $\pi$ , respectively. This shows that the slopes are perpendicular to each other as can be seen from Fig. 2.

When the total phase difference  $2(\chi_2 - \chi_0)$  across the SNS is sandwich is calculated as defined by Eq. (32), the contribution from the  $S$  regions modify the current phase relation from that shown in Fig. 2. Although the phase difference is defined differently in Ref. 13 from that of Eq. (32), the results of Ref. 14 show a current phase relation which is different from that of the Josephson relation<sup>7</sup> in the weak coupling limit. It is not obvious why such a deviation from the Josephson relation should exist.

### VI. MEASURED CURRENT DENSITY AND JOSEPHSON PENETRATION

When one of the dimensions of the SNS specimen transverse to the current flow is larger than the Josephson penetration depth the current density is nonuniform over the cross section of the specimen. We therefore have to include effects due to nonuniform currents in our results when comparing theory with experiments to which nonuniform current densities may apply. In a large superconductor the current flows near the surface over a depth  $\lambda_s$  and in the  $N$  region that depth is  $\lambda_J$ . Since in our normalized units  $\kappa^2 \nabla \times \nabla \times (\nabla \chi) = \vec{1} = -f^2 \nabla \chi \approx -\vec{1}_c \sin[2(\chi_2 - \chi_1)]$  in the weak coupling limit, we may replace approximately  $(\nabla \chi)_x$  by  $[\chi_2(y) - \chi_1(y)] / (\lambda_s + d_n)$ , where  $y$  is the normalized coordinate perpendicular to the current flow and  $\kappa = \lambda_s / \xi_s$ . The point 1 is chosen a distance  $\lambda_s$  ( $\lambda_s / \xi_s$  in our normalization) from the  $SN$  boundary in the  $S$  region, and the point 2 is in the center of the  $N$  region.

We assume that the gradient of  $\chi$  has no  $x$  dependence. Therefore,  $\nabla \cdot [\nabla\chi(y)]$  is zero and

$$\frac{\kappa^2 \partial^2 \Delta\chi_{12}}{\partial y^2} \approx i_c (\lambda_s + d_n) \sin(2\Delta\chi_{12}). \quad (34)$$

In the *low-current limit*, when  $\sin(2\Delta\chi_{12})$  is replaced by  $2\Delta\chi_{12}$ , one obtains from Eq. (34) a solution  $\Delta\chi_{12} = (\Delta\chi_{12})_0 e^{-y/\lambda_J}$  with  $\lambda_J$  the usual Josephson penetration depth<sup>19</sup> in the  $N$  region which is in esu units:

$$\lambda_J = \left( \frac{c\phi_0}{16\pi^2} \frac{1}{J_c(d_n + \lambda_s)} \right)^{1/2}. \quad (35)$$

If the cross-sectional area of the  $N$  region is  $w^2$  and  $\lambda_J < \frac{1}{4}w$ , then the supercurrent will flow near the surface of the  $N$  region through a cross-sectional area of approximately  $4w\lambda_J$  with approximately uniform current density  $J_s$ . It is assumed that Eq. (35) is also approximately correct when  $J_s = J_c$ . Then the *apparent measured* critical current density  $J_{cm}$  is ( $I_{cm}$  is the measured critical current)  $J_{cm} = I_{cm}/w^2 = J_c 4w\lambda_J/w^2$ , where  $J_c$  is the critical current density given by Eq. (31). Therefore for  $\lambda_J < \frac{1}{4}w$  the value of the measured critical current density  $J_{cm}$  in esu units becomes

$$J_{cm} = \frac{4}{w} \left( \frac{c\phi_0}{16\pi^2} \frac{J_c}{(d_n + \lambda_s)} \right)^{1/2}. \quad (36)$$

One can also find an exact solution of Eq. (34) for arbitrary current densities when  $w \gg \lambda_J$ . Assuming that the maximum lossless current density  $J_c$  is reached when the phase difference at the surface of the  $N$  region across it is  $2\Delta\chi_{12} = \frac{1}{2}\pi$ , we find in terms of Clausen's or Lobachevskiy's function that at  $J_c$  the penetration depth  $\lambda_J$  is increased by 3.6% compared to that of the low-current-density limit [Eq. (35)].

One may also speculate that it might be possible to go to larger phase differences at the surface of the  $N$  region, maybe even up to  $2\Delta\chi_{12} = \pi$ . In that case the current density at the surface would decrease while the maximum lossless current density would move into the  $N$  region away from the surface until at  $2\Delta\chi_{12} = \pi$  the current density at the surface would be zero while at some point below the surface it reaches the maximum value of  $J_c$  and then decreases to zero towards the center of the  $N$  region. Such a solution is mathematically possible from Eq. (34) although physically unlikely to occur in the experiments.<sup>1-4</sup>

## VII. COMPARISON OF THEORY AND EXPERIMENT

Clarke's experiments<sup>2</sup> extend over a wide range of temperatures for a representative number of specimens whose thicknesses of the normal layers range from about 2000 to 7000 Å. We shall com-

pare our theory with some of the results shown in his Figs. 13-15.

We use the following relations and parameters for the S metal:

$$\xi_s = 0.74 [\xi_0 \xi_p / (1 - T/T_c)]^{1/2}, \quad (37)$$

$$\xi_p^{-1} = \xi_0^{-1} + l_s^{-1}. \quad (38)$$

The transition temperature  $T_c$  is obtained by extrapolation of the experimental results to  $J_c = 0$ . The  $T_c$  values differ slightly from specimen to specimen and it is indicated on our figures when a comparison is made near  $T_c$  such as 7 K. Our results below 6.5 K are not affected by a slight variation of  $T_c$  within the accuracy of our comparison.

For Pb the value of  $\xi_0 = 830$  Å. Although the mean free paths  $l_s$  and  $l_n$  were measured<sup>2</sup> to an accuracy of  $\pm 20\%$ , the values of the mean free paths as stated in Ref. 2, were used in the calculations without any adjusting.

$$\lambda_s = \lambda_L(0) / [2\chi_{GS}(1 - T/T_c)]^{1/2}, \quad (39)$$

where  $\lambda_L(0) = 390$  Å,  $\rho_s = \hbar v_{Fs} / 2\pi k T l_s$ ,  $v_{Fs} = 0.434 \times 10^8$  cm/sec,  $l_s = 10^4$  Å, and

$$\chi_{GS}^{-1} \approx 1 + 7\zeta(3)\rho_s/\pi^2. \quad (40)$$

For the normal metal (copper) we used in general

$$|\xi_n| = (\frac{1}{3}\xi_T \xi_{PT})^{1/2}, \quad (41)$$

$$\xi_{PT}^{-1} = (3\xi_T)^{-1} + l_n^{-1}, \quad (42)$$

with  $\xi_T = \hbar v_{Fn} / 2\pi k T$  and  $v_{Fn} = 1.13 \times 10^8$  cm/sec,

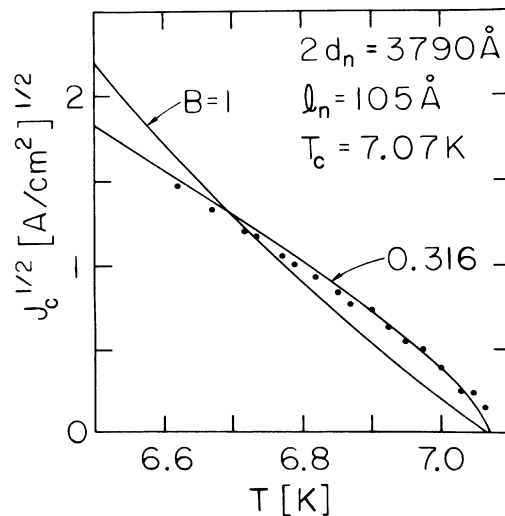


FIG. 3. Solid lines show solutions of the critical current density [Eq. (31)] as a function of temperature near  $T_c$  for two values of the boundary condition  $B$  [Eq. (12)] at the  $SN$  interface. The experimental points are from Ref. 2, Fig. 13.

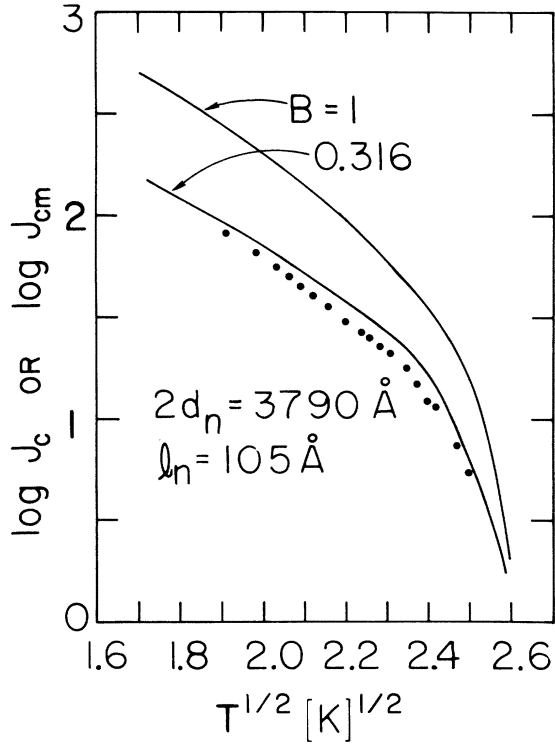


FIG. 4. Shown is the same specimen as in Fig. 3 for lower temperatures. The experimental points are taken from Ref. 2, Fig. 14. The current densities  $J_c$  and  $J_{cm}$  are in  $A/cm^2$ ,  $J_c$  signifies a uniform current density in the  $N$  region [Eq. (31)] and  $J_{cm}$  refers to nonuniform current flow through the  $N$  layer [Eq. (36)] which occurs for the larger current densities. For details, see text. The base of the logarithm is 10.

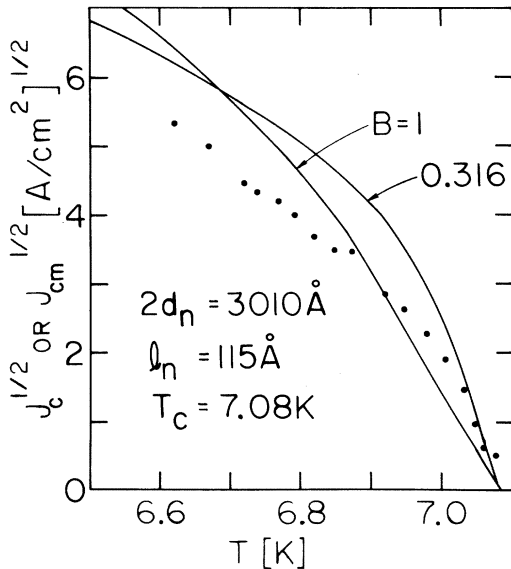


FIG. 5. Similar to Fig. 3 except for a thinner  $N$  layer. For the larger current densities the current flow across the  $N$  layer is nonuniform as in Fig. 4. The experimental points are from Ref. 2, Fig. 13. For details, see text.

$$\chi_{G_n}^{-1} \approx 1 + 7\zeta(3)\rho_n/\pi^2, \quad (43)$$

with  $\rho_n = \hbar v_{F_n}/2\pi k T l_n$ . Equations (41) and (42) with the definitions for  $\xi_T$  assume implicitly that the transition temperature of the  $N$  metal in the bulk  $T_{cn} = 0$ .

Since Cu is dirty in Ref. 2, one can check our results for Cu with  $T_{cn} \neq 0$ . In the dirty limit de Gennes<sup>5</sup> gives an expression for  $|\xi_n|$  when  $T/T_{cn} \gg 1$ :

$$|\xi_n| = (\frac{1}{3}\xi_T l_n)^{1/2} \{1 - 2/[1.39 + \ln(T/T_{cn})]\}^{-1/2}. \quad (44)$$

We have evaluated our results with both equations, namely Eqs. (41) and (44), with the assumption that for Cu the value of  $T_{cn} = 10^{-6}$  K in Eq. (44). Although the differences in the final results of  $J_c$  were not very large, the overall fit to the experimental results indicated that Eq. (41) is most likely the better of those two choices. The figures shown below are calculated with Eq. (41).

Figure 3 shows a plot of the square root of the critical current density  $J_c$ , Eq. (31), as a function of temperature when the  $N$  metal is 3790 Å thick, the mean free path in the  $N$  metal  $l_n = 105$  Å and  $T_c = 7.07$  K. The solid curves are calculated with  $B = |\Delta_{G_n}|/|\Delta_{G_s}| = 1$  and 0.316 at the SN boundaries. The reader should be reminded that  $\Delta_{G_n}$  is an effective pair potential, induced by the proximity effect in the  $N$  metal, as explained in Sec. II. Obviously, the temperature dependence of  $\sqrt{J_c}$  depends on the boundary conditions at the SN interface. There are no adjustable parameters in the calculations except the boundary condition  $B$ . We shall comment on  $B$  below.

Figure 4 shows the temperature dependence of the critical current of the same specimen as shown in Fig. 3 for lower temperatures. The solid lines are calculated with  $B = 1$  and  $B = 0.316$  from Eq. (31) and Eq. (36), where the latter current density is the apparent measured critical current density  $J_{cm}$  due to nonuniform current flow through the  $N$  metal. The smaller one of both current values is plotted at a fixed temperature. For higher temperatures it is the value  $J_c$  [Eq. (31)] that is shown and for lower temperatures it is  $J_{cm}$  [Eq. (36), with  $w = 0.02$  cm] that is plotted. Again, the boundary condition  $B = 0.316$  gives a good fit to the experimental results of Ref. 2, Fig. 14, shown by the solid points. No other parameters are adjusted.

Figure 5 is similar to Fig. 3 for a specimen with a thinner copper layer. For current densities larger than about 15  $A/cm^2$  the value of  $J_{cm}$  is plotted, indicating nonuniform current flow. The experimental points (Ref. 2 Fig. 13) of the current density follow the temperature dependence of the



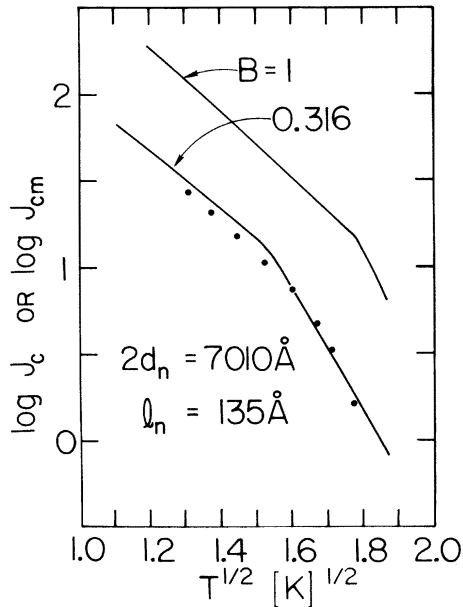


FIG. 6. Similar to Fig. 4 except for a thick  $N$  layer. The experimental points are from Ref. 2, Fig. 14. Current densities are in  $\text{A}/\text{cm}^2$ . The base of the logarithm is 10.

calculated results with boundary condition  $B \approx 0.316$ . A slightly smaller  $B$  value might lead to a better fit to the experimental results.

Figure 6 is a comparison of the temperature de-

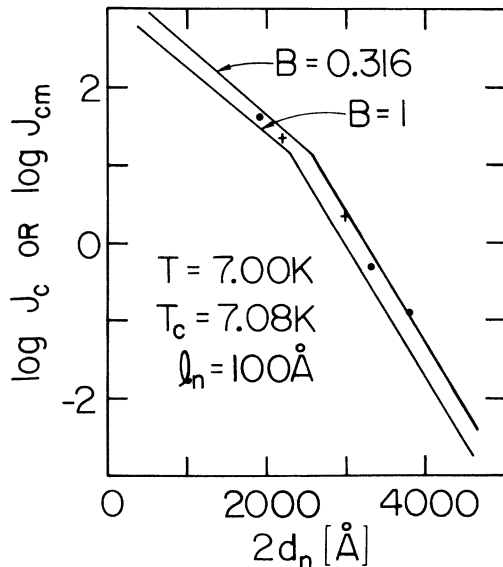


FIG. 7. Thickness dependence of the critical current densities  $J_c$  [Eq. (31)] or  $J_{cm}$  [Eq. (36)] for a constant temperature of 7 K. The solid lines are calculated with a mean free path of  $100 \text{ \AA}$  in the  $N$  metal and  $10^4 \text{ \AA}$  in the  $S$  metals. The experimental points and crosses which have mean free paths close to these values are taken from Ref. 2, Fig. 15. Current densities are in  $\text{A}/\text{cm}^2$ . The base of the logarithm is 10.

pendence of the critical current density for a thick  $N$  layer at low temperatures. The experimental points are taken from Ref. 2, Fig. 14. Again, boundary condition  $B=0.316$  seems to give a reasonable fit of our theory to the experiments.

Figures 7 and 8 show the thickness dependences of the critical current densities at constant temperatures and the experimental points and crosses are taken from Ref. 2, Fig. 15. The solid lines at  $T=7 \text{ K}$  were computed with  $T_c=7.08 \text{ K}$ ,  $l_n=100 \text{ \AA}$ , and  $l_s=10^4 \text{ \AA}$ . Each experimental point, however, had slightly different  $T_c$  and  $l_n$  values. The chosen  $T_c$  and  $l_n$  values for the solid lines are average values and the exact fit of theory and experiment at  $T=7 \text{ K}$  depends on the exact choice of  $T_c$  since  $T$  is very close to  $T_c$ . This problem does not arise in Fig. 8, since at  $T=3 \text{ K}$  the exact value of  $T_c$  does not change the calculated curves. In Fig. 8, the average mean free paths used in the calculation were  $l_n=135 \text{ \AA}$  and  $l_s=10^4 \text{ \AA}$ .

We have compared our theory to the experimental results by adjusting the boundary conditions of the pair potential [Eq. (12)] at the  $SN$  interfaces. We have also used various other values of  $B$ , not shown in the figures. For most specimens of Ref. 2, a constant value of  $B \approx 0.316$  gave a reasonable fit over all temperatures and thicknesses investigated. We compared also our theory with the experimental results by making  $\gamma$  constant [Eq. (11)]. Although in certain temperature ranges and particularly for  $T=\text{constant}$ , as for example in Figs. 7 and 8, we were able to fit reasonably the theory to the experiments, the overall fit for all temperatures investigated was by far better for  $B$  a constant than  $\gamma$  a constant. Thus, the continuity or discontinuity of the pair potential as the  $SN$  interfaces [Eq. (12)] is the important parameter

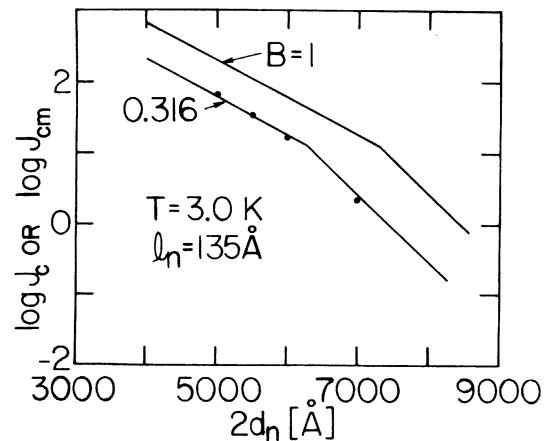


FIG. 8. Similar to Fig. 7 except for  $T=3 \text{ K}$ . The experimental points are taken from Ref. 2, Fig. 15. Current densities are in  $\text{A}/\text{cm}^2$ . The base of the logarithm is 10.

which controls the critical current density and not that of the order parameters [Eq. (11)] for all temperatures and thicknesses investigated.

### VIII. BOUNDARY CONDITIONS

The continuity of the phase current density at the  $SN$  boundary leads to relation (5a) with the value of  $b$  [Eq. (12)] unspecified. Our solution would be completely specified if  $b \equiv B^2$  were known.

Zaitsev<sup>20</sup> considered the boundary conditions of the pair potential at the  $SN$  interface from the microscopic point of view for two superconductors whose transition temperatures in bulk form,  $T_{cs}$  and  $T_{cn}$ , are not too far apart. At a temperature  $T$  between  $T_{cn}$  and  $T_{cs}$  he finds that the pair potential  $\Delta_G$  is continuous for specular electron reflections and  $mv_F \Delta_G$  for diffuse electron reflections at the  $SN$  boundary such that

$$B_{sp} = 1 \quad (45)$$

and

$$B_{diff} = (m_s/m_n)(v_{Fs}/v_{Fn}). \quad (46)$$

De Gennes<sup>5</sup> finds that  $\Delta_G/N(0)V$  is generally continuous from which it follows that

$$B_{DG} = N_n(0)V_n/N_s(0)V_s. \quad (47)$$

Since  $l_s/\sigma_s = 1.056 \times 10^{-11} \Omega \text{ cm}^2$  for Pb and  $l_n/\sigma_n = 0.651 \times 10^{-11} \Omega \text{ cm}^2$  for Cu, where  $\sigma$  is the conductivity it follows from the free-electron theory that  $m_n/m_s = 0.481$  and  $n_s/n_n = 0.484$ . Therefore, one obtains for Pb-Cu the values  $B_{diff} = 0.799$  and  $B_{DG} = 0.139$ , the latter for  $T_{cn} = 10^{-6}$  K. The  $B$  value found by comparing our theory with Clarke's experiments is  $B \approx 0.316$ . We have also compared the experimental results<sup>2</sup> with our theory using  $B_{DG} = 0.139$  and found that we could not get agreement with that boundary condition.

Assuming that Zaitsev's boundary conditions can be applied to the Pb-Cu system, say  $B_{diff}$ , then we find that the experimentally obtained  $B$  value corresponds to a  $\Delta_{Gn}$  at the  $SN$  boundary which is smaller than that predicted by  $B_{diff}$  by a factor of about 2.5, but larger than that predicted by  $B_{DG}$  by a factor of about 2.3. From the experimental-point of view it seems certainly easier to justify a decrease of  $\Delta_{Gn}$  at the  $SN$  interface due to impurities (oxide layer) introduced in the evaporation process of the SNS layers than it is to justify an enhancement of  $\Delta_{Gn}$ .

Assuming de Gennes's boundary condition were to apply such that  $B_{DG} = B = 0.316$ . One then obtains from Eq. (47), a value of  $N_n(0)V_n$  which corresponds to a transition temperature of Cu of about 0.05 K. This cannot be correct and therefore, as pointed out above,<sup>18</sup> one must interpret  $\Delta_{Gn}$  as an

induced pair potential in the  $N$  metal which arises from the  $S$  metal and not that due to the intrinsic  $N_n(0)V_n$  interaction in Cu. Therefore, one cannot draw any conclusion from the experiments regarding the intrinsic  $N_n(0)V_n$  interaction of copper, at least not to first approximation because the induced  $\Delta_{Gn}$  is much larger than its intrinsic value.

### IX. CONCLUSIONS

We derived a general equation for the maximum lossless current density  $J_c$  [Eq. (31)] which can be sustained across a symmetric SNS triple layer provided the thicknesses of the  $S$  layers are larger than  $\xi_s$  and the thickness of the  $N$  layer  $2d_n \gtrsim |\xi_n|$ . No restrictions are made concerning the clean or dirty limits of the  $S$  and  $N$  metals. The value of  $J_c$  depends also on the boundary condition  $B$  [Eq. (12)] which is a measure of how well the pair potentials at the  $SN$  boundaries are matched. The premultiplier of the exponential term of Eq. (31) has in general a rather complicated temperature dependence which is linked implicitly to the boundary conditions at the  $SN$  interfaces. The premultiplier is also proportional to  $(T - T_c)^n$  where  $n$  may vary from 1 to 2. The exponent of the exponential term is also temperature dependent through  $|\xi_n|$  [Eqs. (41) or (44)]. Equation (31) was adapted to nonuniform current flow across the  $N$  metal [Eq. (36)].

Equations (31) and (36) were compared to experiments by Clarke<sup>2</sup> (Figs. 3-8). The restriction  $d_s > \xi_s$  is always satisfied in Ref. 2 for  $T \leq 7$  K. We found that agreement between theory and experiment can be obtained over a wide range of temperatures and thicknesses of the  $N$  layer provided we let the ratio of the pair potentials at the  $SN$  boundaries  $|\Delta_{Gn}|/|\Delta_{Gs}| \equiv B$  be a constant for a given SNS specimen. We find  $B \approx 0.3$  for all the specimens investigated. This might be rather fortuitous and the exact value of  $B$  is probably, within limits, not of significance since  $B$  might depend on the cleanliness of sample preparation. The temperature independence of  $B$  for a given specimen is, however, of significance since it tells us that the ratio of the pair potentials at the  $SN$  boundaries does not vary with temperature (for example, Figs. 3 and 4). This implies that the pair potentials in the  $S$  and  $N$  regions have the same temperature dependences. It appears also that this ratio is independent of the thickness of the  $N$  layer, at least to first approximation (Figs. 7 and 8).

In the present theory  $\Delta_{Gn}$  is interpreted as an effective pair potential in copper, induced to first approximation by the proximity effect of Pb in Cu, and not that due to the intrinsic electron-photon

interaction which Cu might possess in bulk form. The latter is probably much smaller than the former which is corroborated by the fact that  $\Delta_{G_n}$  and  $\Delta_{G_s}$  at the NS boundaries have the same temperature dependences ( $B = \text{const}$ ).

The square of the order parameter (superelectron density) in the center of the  $N$  region is finite (not zero) for all current densities including the critical current density [Eq. (21b)]. Its value at the critical current density is 50% of its zero-current value.

The thickness dependence of the phase difference of the order parameters across the  $N$  region is given by Eq. (33b) and Fig. 2 as a function of current. When the  $N$  layer becomes thick compares to  $|\xi_n|$ , e.g.,  $2d_n/|\xi_n| \gtrsim 3$ , one approaches the very weak coupling limit in which case Eq. (33b) reduces to the Josephson dc current relation, Eq.

(33c). When the thickness of the  $N$  layer is reduced, the phase difference across the  $N$  layer is less than  $\frac{1}{2}\pi$  at the critical current density as the two S sides couple more strongly.

Preliminary exact computer solutions for the general case confirm the accuracy of the above analytic approximation. The complete numerical results will be published separately<sup>21</sup> in Paper II.

#### ACKNOWLEDGMENTS

I am obliged to R. S. Poulsen for his help with the numerical results related to the figures, and to Professor K. H. Bennemann, Freie Universität Berlin, for his hospitality during my short stay at his Institute where some of the results of this paper were obtained. I am also obliged to the German Academic Exchange Service (DAAD) for making this visit possible.

\*Supported in part by National Science Foundation Grant No. ENG73-08279 A01 and a faculty research grant from the University of California, Davis, California 95616.

<sup>1</sup>H. Meissner, Phys. Rev. **117**, 672 (1960).

<sup>2</sup>J. Clarke, Proc. R. Soc. A **308**, 447 (1969).

<sup>3</sup>S. I. Bondarenko, I. M. Dmitrenko, and E. I. Balanov, Fiz. Tverd. Tela **12**, 1417 (1970) [Sov. Phys.-Solid State **12**, 1113 (1970)].

<sup>4</sup>A. Gilabert, J. P. Laheurte, J. P. Romagnan, and J. C. Noiray, in *Fourteenth International Conference on Low Temperature Physics* (North-Holland, Amsterdam, 1975), Vol. 4, pp. 92-95.

<sup>5</sup>P. G. de Gennes, Rev. Mod. Phys. **36**, 225 (1964).

<sup>6</sup>K. Yamafuji, T. Ezaki, and T. Matsushita, J. Phys. Soc. Jpn. **30**, 965 (1971); K. Yamafuji, T. Ezaki, T. Matsushita and F. Irie, in *Proceedings of the Twelfth International Conference on Low Temperature Physics, Kyoto*, edited by E. Kauda (Academic, Kyoto, 1970).

<sup>7</sup>B. D. Josephson, Phys. Lett. **1**, 251 (1962); Adv. Phys. **14**, 419 (1965).

<sup>8</sup>D. A. Jacobson, Phys. Rev. **138**, A1066 (1965).

<sup>9</sup>V. L. Ginzburg and L. D. Landau, Zh. Eksp. Teor. Fiz. **20**, 1064 (1950).

<sup>10</sup>O. Kulik, Zh. Eksp. Teor. Fiz. **57**, 1745 (1969) [Sov. Phys.-JETP **30**, 944 (1970)].

<sup>11</sup>C. Ishii, Prog. Theor. Phys. **44**, 1525 (1970); in *Pro-*

*ceedings of the Twelfth International Conference on Low Temperature Physics, Kyoto*, edited by E. Kauda (Academic, Kyoto, 1970), pp. 435 and 436.

<sup>12</sup>J. Bardeen and J. L. Johnson, Phys. Rev. B **5**, 72 (1972).

<sup>13</sup>A. Baratoff, J. A. Blackburn, and B. B. Schwartz, Phys. Rev. Lett. **25**, 1096 (1970); **25**, 1738(E) (1970).

<sup>14</sup>J. A. Blackburn, B. B. Schwartz, and A. Baratoff, J. Low Temp. Phys. **20**, 523 (1975).

<sup>15</sup>L. P. Gor'kov, Zh. Eksp. Teor. Fiz. **37**, 1407 (1959) [Sov. Phys.-JETP **10**, 998 (1960)].

<sup>16</sup>H. J. Fink, M. Sheikholeslam, A. Gilabert, J. P. Laheurte, J. P. Romagnan, J. C. Noiray, and E. Guyon, this issue, Phys. Rev. B **14**, 1052 (1976).

<sup>17</sup>M. Abramowitz and I. A. Stegun, *Handbook of Mathematical Functions* (U.S. Nat. Bur. Stand., Washington, D.C., 1968), Eq. 17.4.51.

<sup>18</sup>P. F. Byrd and M. D. Friedman, *Handbook of Elliptic Integrals for Engineers and Physicists* (Springer, Berlin, 1954), Eq. 339.01.

<sup>19</sup>R. A. Ferrell and R. E. Prange, Phys. Rev. Lett. **10**, 479 (1963); P. W. Anderson, in *Lectures on the Many-body Problem*, edited by E. R. Caianiello (Academic, New York, 1964); B. D. Josephson, Rev. Mod. Phys. **36**, 216 (1964).

<sup>20</sup>R. O. Zaitsev, Zh. Eksp. Teor. Fiz. **50**, 1055 (1966) [Sov. Phys.-JETP **23**, 702 (1966)].

<sup>21</sup>R. S. Poulsen and H. J. Fink (unpublished).